

The Performance Analysis of Spectrum Sharing between UAV enabled Wireless Mesh Networks and Ground Networks

Zhiqing Wei, Jialin Zhu, Zijun Guo, and Fan Ning

Abstract—Unmanned aerial vehicle (UAV) has the advantages of large coverage and flexibility, which could be applied in disaster management to provide wireless services to the rescuers and victims. When UAVs forms an aerial mesh network, line-of-sight (LoS) air-to-air (A2A) communications have long transmission distance, which extends the coverage of multiple UAVs. However, the capacity of UAV is constrained due to the multiple hop transmissions in aerial mesh networks. In this paper, spectrum sharing between UAV enabled wireless mesh networks and ground networks is studied to improve the capacity of UAV networks. Considering two-dimensional (2D) and three-dimensional (3D) homogeneous Poisson point process (PPP) modeling for the distribution of UAVs within a vertical range Δh , stochastic geometry is applied to analyze the impact of the height of UAVs, the transmit power of UAVs, the density of UAVs and the vertical range, etc., on the coverage probability of ground network user and UAV network user. Besides, performance improvement of spectrum sharing with directional antenna is verified. With the object function of maximizing the transmission capacity, the optimal altitude of UAVs is obtained. This paper provides a theoretical guideline for the spectrum sharing of UAV enabled wireless mesh networks, which may contribute significant value to the study of spectrum sharing mechanisms for UAV enabled wireless mesh networks.

Index Terms—Unmanned Aerial Vehicle; Aerial Mesh Networks; Spectrum Sharing.

I. INTRODUCTION

UAV enabled wireless communication has unique advantages of long signal propagation distance and flexible deployment [1], which has attracted wide attention. Among the applications of UAVs, UAV-mounted BSs can establish wireless connections for mobile devices in disaster management [2] and offload traffic from ground base stations (BSs) with heavy traffic load [3].

Multiple UAVs can provide wireless services efficiently [2]. Chand *et al.* [4] proposed a framework of UAV mesh network to support disaster management and military operations. Lyu *et al.* [6] designed a geometrical UAV placement method to serve the ground users with minimum number of UAVs. Bor-Yaliniz *et al.* [7] designed a UAV placement method considering

An earlier version of this paper was presented at the WCSP 2018 Conference and was published in its Proceedings [26]. The URL of this conference paper is: <https://ieeexplore.ieee.org/document/8555855>. This work was supported in part by the Beijing Natural Science Foundation (No. L192031) and the National Natural Science Foundation of China under Grant 61631003.

Zhiqing Wei, Jialin Zhu, Zijun Guo, and Fan Ning are with Key Laboratory of Universal Wireless Communications, Ministry of Education, Beijing University of Posts and Telecommunications, Beijing 100876, China (email: {weizhiqing, jialinzhu, zijunguo, ningfan}@bupt.edu.cn).

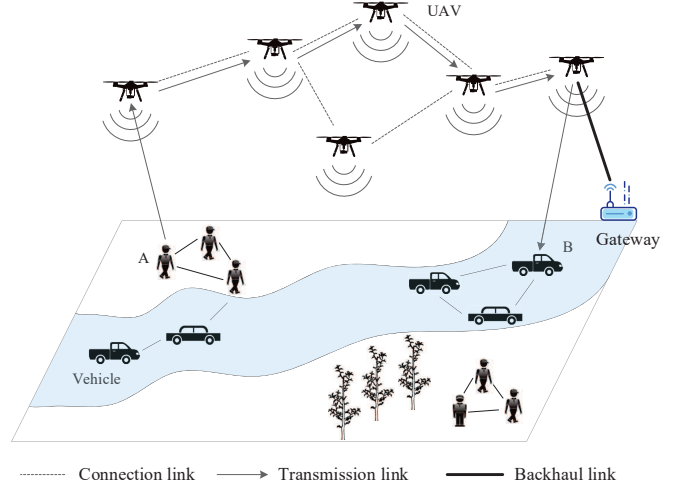


Fig. 1. The application scenario of UAV mesh network.

environment parameters such as shapes of buildings. Plachy *et al.* [8] jointly optimized placement of UAV-mounted BSs and user association scheme. Lu *et al.* [9] designed a measurement-aided dynamic planning to optimize placement and channel allocation of UAV-mounted BSs. In [10], a UAV mesh network is developed by our team. The scenario of [10] is illustrated in Fig. 1, where the UAV mesh network provides connections for ground users.

According to [11], as the number of nodes increases, the capacity of wireless mesh networks decreases dramatically because of the existence of the multiple hop transmissions. As illustrated in Fig. 1, the per-node capacity is limited because of multiple hop transmissions [12] in the aerial tier of UAV mesh networks. Fortunately, there is spatial separation between UAV mesh networks and ground networks [13]. Besides, in disaster management, most of ground BSs are destroyed and the density of ground BS is small, which creates the opportunity for UAVs to share the spectrum of ground networks. In such way, the capacity of UAV mesh networks can be improved. Actually, the study of the spectrum sharing for UAV networks is initiated. Zhang *et al.* [14], [15] initially allowed drone small cell networks to share the spectrum of cellular networks. Lyu *et al.* [16] proposed an orthogonal spectrum sharing scheme for UAV networks. The spectrum sharing between UAV and radar was studied in [17]. The power control in cognitive UAV networks was studied in [18] to optimize energy efficiency. Huang *et al.* [19] studied the protocol design in cognitive aerial

TABLE I
KEY PARAMETERS AND NOTATIONS

Symbol	Description
P_u	Transmit power of UAV
P_d	Transmit power of TXs of ground network
λ_d	TXs density of ground network
λ_{2Du}	User density of 2D UAV network
λ_{3Du}	User density of 3D UAV network
h_1	Minimum height of 3D UAV network
Δh	Vertical range of 3D UAV network
α_d	Path-loss exponent of ground-to-ground link
α_u	Path-loss exponent of air-to-ground link
N	Variance of additive white Gaussian noise
η	Attenuation factor due to NLoS propagation
β	SINR threshold
B and C	Environmental dependent constants
θ	Elevation angle of air-to-ground link by line-of-sight transmission
γ_{gu}	Received SINR of typical ground network user
γ_{uu}	Received SINR of UAV network user
I_{gu}^c	Interference generated by TXs of ground network
I_u	Interference generated by TXs of UAV network
I_u^c	Received interference from TXs of UAV network
P_1	Coverage probability of typical ground network user
P_2	Coverage probability of typical UAV network user
$L_A(*)$	Laplace transform of random variable A
g_0	Small scale fading gain between typical ground network user and its associated TX
g_i	Small scale fading gain of i th interference link
d_0	Distance between typical ground network user and its associated TX
d_i	Distance between i th BS of ground network and the user at the origin $\{\mathbf{0}\}$
x_0	Distance between typical UAV network user and its associated UAV
x_i	Distance between i th UAV and the user at the origin $\{\mathbf{0}\}$

networks. Wang *et al.* [20] addressed the trajectory planning and spectrum sharing scheme for cognitive UAV networks.

Although the spectrum sharing of UAV networks was studied, very few of literatures studied spectrum sharing between UAV mesh networks and ground networks. In this paper, considering two-dimensional (2D) and three-dimensional (3D) deployment of UAVs, we study the spectrum sharing between the A2A communications of UAVs and ground networks to enhance the capacity of A2A communications. The coverage performance of UAV mesh network is analyzed applying the stochastic geometry. Directional antennas are employed to improve coverage performance of UAV mesh network. The performance improvement using directional antennas is compared with UAV network using omnidirectional antennas. Finally, with the object function of maximizing transmission capacity, the optimal altitude of UAVs is obtained. It is noted that part of this work was published in WCSP 2018 [26]. The novel contributions include study of spectrum sharing with 2D UAV network, directional A2A and air-to-ground (A2G) transmission, and the transition from 3D UAV network to 2D UAV network. Specifically, we discover that derived results of 3D UAV network transit to that of 2D UAV network when the vertical range of 3D UAV deployment tends to 0. Finally,

more comprehensive simulation results are provided in this paper compared with the conference paper. Hence, this paper provides a complete study for spectrum sharing of UAV mesh networks.

The rest of this paper is organized as follows. In Section II, the system model of this paper is introduced. The spectrum sharing of UAV networks with omnidirectional transmission is analyzed in Section III. The coverage probabilities of UAV and ground networks with directional transmission are derived in Section IV. The numerical results and analysis are provided in Section V. Finally, Section VI provides the conclusion. The key parameters and notations are listed in Table I.

II. SYSTEM MODEL

A. Network model

As illustrated in Fig. 2 and Fig. 3, 2D and 3D deployment of UAVs are considered. For 2D scenario, the distributions of the UAVs and transmitters (TXs) of ground network follow 2D homogeneous PPP with densities λ_{2Du} and λ_d , respectively. The UAVs are deployed above the ground with height h . In 3D scenario, the distribution of TXs of ground network is the same to the scenario in Fig. 2. The UAVs are distributed following a 3D homogeneous PPP with density λ_{3Du} . UAVs

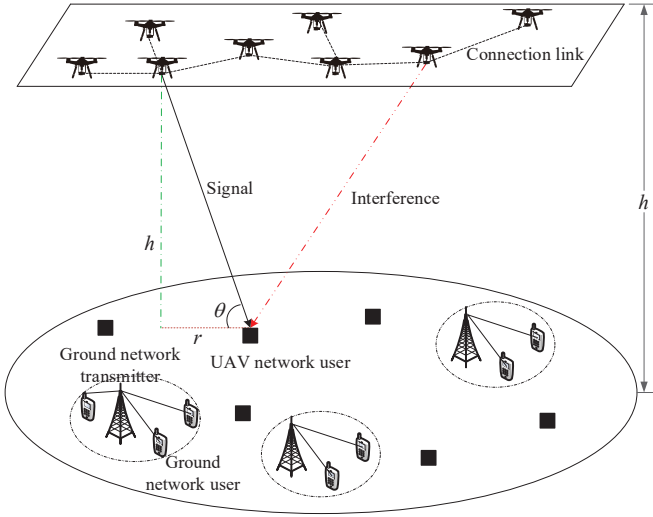


Fig. 2. 2D deployment of UAVs.

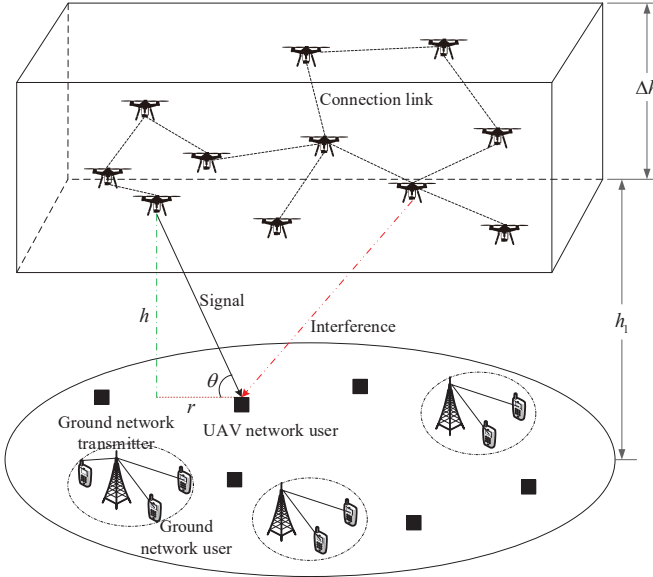


Fig. 3. 3D deployment of UAVs.

are deployed in the space between two planes with heights h_1 and $h_1 + \Delta h$, respectively.

B. Channel model

Path-loss exponents of ground-to-ground (G2G) and A2G links are α_d and α_u , respectively. The power gain of small scale fading is modeled using an exponentially distributed random variable with unit mean. A Gaussian distribution random variable with mean zero and variance N is used to model the power of additive white Gaussian noise. UAV and TX of ground network transmit with power P_u and P_d , respectively. The received power of UAV network user in the cases of line-of-sight (LoS) and non-line-of-sight (NLoS) transmissions is [21], [24]

$$P_{r,g} = \begin{cases} P_u |d_{ug}|^{-\alpha_u} & \text{LoS} \\ \eta P_u |d_{ug}|^{-\alpha_u} & \text{NLoS} \end{cases}, \quad (1)$$

where η is a diminution factor [21] and d_{ug} is the distance between UAV and the associated user. The A2G link is LoS with probability [21].

$$P_{\text{LoS}} = \frac{1}{1 + C \exp(-B(\theta - C))}, \quad (2)$$

where θ is the elevation angle, B and C are environment dependent constants.

C. Directional antenna model

Directional antennas are applied in A2A and A2G links to reduce interference. The antenna gain expressed in the unit of dB is [22], [23]

$$G(\alpha, \theta_{-3dB}) = \begin{cases} G_0 - 3.01 \cdot \left(\frac{2\alpha}{\theta_{-3dB}}\right)^2, & 0^\circ \leq \alpha \leq \frac{\theta_{ml}}{2}, \\ G_{sl}, & \frac{\theta_{ml}}{2} \leq \alpha \leq 180^\circ, \end{cases}$$

$$G_0 = 10 \log\left(\left(\frac{1.6162}{\sin(\theta_{-3dB}/2)}\right)^2\right),$$

$$\theta_{ml} = 2.6 \cdot \theta_{-3dB},$$

$$G_{sl} = -0.4111 \cdot \ln(\theta_{-3dB}) - 10.597, \quad (3)$$

where G_0 is the maximum antenna gain, G_{sl} is the antenna gain of side lobe, θ_{-3dB} is the half power bandwidth of directional antenna, α is the angle between the line connecting TX and receiver (RX) and the center line of transmit beam, and θ_{ml} is the angle of main lobe.

III. SPECTRUM SHARING WITH OMNIDIRECTIONAL TRANSMISSION

In order to study the characteristics of spectrum sharing between UAV mesh networks and ground networks, we introduce the concept of the coverage probability. The coverage probability is defined as the probability of successful communication for ground network user and UAV network user. In this paper, considering that UAV network users and ground network users are the same type of users, the threshold of signal-to-interference-plus-noise ratio (SINR) for successful communication is the same, denoted by β . P_1 denotes the coverage probability of typical ground network user. Its main interference includes ground network transmitters and UAV networks under spectrum sharing. P_2 denotes the coverage probability of typical UAV network user. The main interference comes from the UAV network air-to-ground communication links.

In this section, with 2D and 3D deployment of UAVs, the performance of spectrum sharing is studied. When $\Delta h \rightarrow 0$, 3D deployment of UAVs reduces to 2D deployment of UAVs. In this situation, we reveal that coverage probability with 3D deployment of UAVs turns into coverage probability with 2D deployment of UAVs.

A. Spectrum sharing of 2D UAV network

1) *Performance of ground network:* For ground network, the signal to interference plus noise ratio (SINR) of the typical

$$L_{I_{gu}^c}\left(\frac{\beta d_0^{\alpha_d}}{P_d}\right) = \exp\left(-\frac{2\lambda_d\pi^2(\beta)^{2/\alpha_d}d_0^2}{\alpha_d \sin(2\pi/\alpha_d)}\right). \quad (4)$$

$$\begin{aligned} L_{I_{u,\text{LoS}}}\left(\frac{\beta d_0^{\alpha_d}}{P_d}\right) &= \exp(-\lambda_2 D_u) \int_V \left(1 - \frac{1}{1 + \frac{\beta d_0^{\alpha_d}}{P_d} P_u P_{\text{LoS}} x_i^{-\alpha_u}}\right) dx \\ &= \exp(-2\pi\lambda_2 D_u) \int_0^\infty \left(1 - \frac{1}{1 + \frac{\beta d_0^{\alpha_d}}{P_d} P_u (\sqrt{r^2 + h^2})^{-\alpha_u} \frac{1}{1+C \exp(-B(\frac{180}{\pi} \arctan(h/r)-C))}}\right) r dr \\ &= \exp(-2\pi\lambda_2 D_u H_1(\beta, d_0, h, \alpha_d, \alpha_u)), \end{aligned} \quad (5)$$

$$\begin{aligned} L_{I_{u,\text{NLoS}}}\left(\frac{\beta d_0^{\alpha_d}}{P_d}\right) &= \exp(-2\pi\lambda_2 D_u) \int_0^\infty \left(1 - \frac{1}{1 + \frac{\beta d_0^{\alpha_d}}{P_d} P_u (\sqrt{r^2 + h^2})^{-\alpha_u} \eta \left(1 - \frac{1}{1+C \exp(-B(\frac{180}{\pi} \arctan(h/r)-C))}\right)}\right) r dr \\ &= \exp(-2\pi\lambda_2 D_u H_2(\beta, d_0, h, \alpha_d, \alpha_u)), \end{aligned} \quad (6)$$

where

$$H_1(\beta, d_0, h, \alpha_d, \alpha_u) = \int_0^\infty \left(1 - \frac{1}{1 + \frac{\beta d_0^{\alpha_d}}{P_d} P_u (\sqrt{r^2 + h^2})^{-\alpha_u} \frac{1}{1+C \exp(-B(\frac{180}{\pi} \arctan(h/r)-C))}}\right) r dr, \quad (7)$$

$$H_2(\beta, d_0, h, \alpha_d, \alpha_u) = \int_0^\infty \left(1 - \frac{1}{1 + \frac{\beta d_0^{\alpha_d}}{P_d} P_u (\sqrt{r^2 + h^2})^{-\alpha_u} \eta \left(1 - \frac{1}{1+C \exp(-B(\frac{180}{\pi} \arctan(h/r)-C))}\right)}\right) r dr. \quad (8)$$

user, namely, the user at the origin $\{\mathbf{0}\}$ is

$$\gamma_{gu} = \frac{P_d d_0^{-\alpha_d} g_0}{I_{gu}^c + I_u + N}, \quad (9)$$

where d_0 denotes the distance between the user at the origin $\{\mathbf{0}\}$ and the associated BS, I_{gu}^c is the aggregated interference received by the typical user from the BSs of ground network, I_u is the aggregated interference received by the typical user from UAVs, and g_0 is the power gain of small scale channel fading between the user at the origin $\{\mathbf{0}\}$ and the associated BS.

$$I_{gu}^c = \sum_{d_i \in \Phi_d \setminus \{\mathbf{0}\}} P_d d_i^{-\alpha_d} g_i, \quad (10)$$

$$\begin{aligned} I_u &= I_{u,\text{LoS}} + I_{u,\text{NLoS}} \\ &= \sum_{x_i \in \Phi_u} P_{\text{LoS}} P_u x_i^{-\alpha_d} g_i + \sum_{x_i \in \Phi_u} (1 - P_{\text{LoS}}) \eta P_u x_i^{-\alpha_d} g_i, \end{aligned} \quad (11)$$

where g_i is the power gain of small scale channel fading of i th interference link, x_i is the distance between i th UAV and the user at the origin $\{\mathbf{0}\}$, and d_i is the distance between i th BS of ground network and the user at the origin $\{\mathbf{0}\}$. For the ground network, the coverage probability of typical user is

$$\begin{aligned} P_1 &= P(\gamma_{gu} > \beta), \\ &= \exp\left(-\frac{\beta d_0^{\alpha_d} (I_{gu}^c + I_u + N)}{P_d}\right) \\ &= \exp\left(-\frac{\beta d_0^{\alpha_d} I_{gu}^c}{P_d}\right) \exp\left(-\frac{\beta d_0^{\alpha_d} I_u}{P_d}\right) \exp\left(-\frac{\beta d_0^{\alpha_d} N}{P_d}\right) \quad (12) \\ &= L_{I_{gu}^c}\left(\frac{\beta d_0^{\alpha_d}}{P_d}\right) L_{I_u}\left(\frac{\beta d_0^{\alpha_d}}{P_d}\right) \exp\left(-\frac{\beta d_0^{\alpha_d} N}{P_d}\right), \end{aligned}$$

where $L_A(*)$ represents Laplace transform of A . With the channel model in (1), we have $I_u = I_{u,\text{LoS}} + I_{u,\text{NLoS}}$. The

Laplace transform of I_u is

$$L_{I_u}\left(\frac{\beta d_0^{\alpha_d}}{P_d}\right) = L_{I_{u,\text{LoS}}}\left(\frac{\beta d_0^{\alpha_d}}{P_d}\right) L_{I_{u,\text{NLoS}}}\left(\frac{\beta d_0^{\alpha_d}}{P_d}\right). \quad (13)$$

Since g_i and PPP are independent, we have

$$\begin{aligned} L_{I_{u,\text{LoS}}}\left(\frac{\beta d_0^{\alpha_d}}{P_d}\right) &= E_{I_{u,\text{LoS}}}[\exp\left(\frac{\beta d_0^{\alpha_d}}{P_d} I_{u,\text{LoS}}\right)] \\ &= E_{g_i, \Phi_u} \left[\prod_{x_i \in \Phi_u \setminus \{\mathbf{0}\}} \exp\left(\frac{\beta d_0^{\alpha_d}}{P_d} g_i P_u P_{\text{LoS}} x_i^{-\alpha_u}\right) \right] \\ &= E_{\Phi_u} \left[\prod_{x_i \in \Phi_u \setminus \{\mathbf{0}\}} E_{g_i}[\exp\left(\frac{\beta d_0^{\alpha_d}}{P_d} P_u P_{\text{LoS}} x_i^{-\alpha_u}\right)] \right] \\ &= E_{\Phi_u} \left[\prod_{x_i \in \Phi_u \setminus \{\mathbf{0}\}} \frac{1}{1 + \frac{\beta d_0^{\alpha_d}}{P_d} P_u P_{\text{LoS}} x_i^{-\alpha_u}} \right], \end{aligned} \quad (14)$$

and

$$\begin{aligned} L_{I_{u,\text{NLoS}}}\left(\frac{\beta d_0^{\alpha_d}}{P_d}\right) &= E_{\Phi_u} \left[\prod_{x_i \in \Phi_u \setminus \{\mathbf{0}\}} \frac{1}{1 + \frac{\beta d_0^{\alpha_d}}{P_d} P_u (1 - P_{\text{LoS}}) \eta x_i^{-\alpha_u}} \right]. \end{aligned} \quad (15)$$

Hence, we have derived $L_{I_u}\left(\frac{\beta d_0^{\alpha_d}}{P_d}\right)$.

$$\begin{aligned} L_{I_u}\left(\frac{\beta d_0^{\alpha_d}}{P_d}\right) &= E_{\Phi_u} \left[\prod_{x_i \in \Phi_u} \frac{1}{1 + \frac{\beta d_0^{\alpha_d}}{P_d} P_u P_{\text{LoS}} x_i^{-\alpha_u}} \right] \\ &\quad \times E_{\Phi_u} \left[\prod_{x_i \in \Phi_u} \frac{1}{1 + \frac{\beta d_0^{\alpha_d}}{P_d} P_u (1 - P_{\text{LoS}}) \eta x_i^{-\alpha_u}} \right]. \end{aligned} \quad (16)$$

The probability generating function of PPP is as follows

$$\begin{aligned}
L_{I_{u,\text{LoS}}^c}\left(\frac{\beta x_0^{\alpha_u}}{P_u}\right) &= \exp(-\lambda_2 D_u \int_V \left(1 - \frac{1}{1 + \beta x_0^{\alpha_u} P_{\text{LoS}} x_i^{-\alpha_u}}\right) dx) \\
&= \exp(-2\pi\lambda_2 D_u \int_0^\infty \left(1 - \frac{1}{1 + \beta x_0^{\alpha_u} (\sqrt{r^2 + h^2})^{-\alpha_u} \frac{1}{1 + C \exp(-B(\frac{180}{\pi} \arctan(h/r) - C))}}\right) r dr) \\
&= \exp(-2\pi\lambda_2 D_u H_3(\beta, x_0, h, \alpha_u)),
\end{aligned} \tag{18}$$

$$\begin{aligned}
L_{I_{u,\text{NLoS}}^c}\left(\frac{\beta x_0^{\alpha_u}}{P_u}\right) &= \exp(-2\pi\lambda_2 D_u \int_0^\infty \left(1 - \frac{1}{1 + \beta x_0^{\alpha_u} (\sqrt{r^2 + h^2})^{-\alpha_u} \eta \left(1 - \frac{1}{1 + C \exp(-B(\frac{180}{\pi} \arctan(h/r) - C))}\right)}\right) r dr) \\
&= \exp(-2\pi\lambda_2 D_u H_4(\beta, x_0, h, \alpha_u)),
\end{aligned} \tag{19}$$

where

$$H_3(\beta, x_0, h, \alpha_u) = \int_0^\infty \left(1 - \frac{1}{1 + \beta x_0^{\alpha_u} (\sqrt{r^2 + h^2})^{-\alpha_u} \frac{1}{1 + C \exp(-B(\frac{180}{\pi} \arctan(h/r) - C))}}\right) r dr, \tag{20}$$

$$H_4(\beta, x_0, h, \alpha_u) = \int_0^\infty \left(1 - \frac{1}{1 + \beta x_0^{\alpha_u} (\sqrt{r^2 + h^2})^{-\alpha_u} \eta \left(1 - \frac{1}{1 + C \exp(-B(\frac{180}{\pi} \arctan(h/r) - C))}\right)}\right) r dr. \tag{21}$$

[14].

$$E\left(\prod_{x_i \in \Phi} f(x)\right) = \exp(-\lambda_d \int_V [1 - f(x)] dx), \tag{17}$$

Hence, we have $L_{I_{gu}^c}\left(\frac{\beta d_0^{\alpha_d}}{P_d}\right)$ as in (4) [25]. $L_{I_u}\left(\frac{\beta d_0^{\alpha_d}}{P_d}\right)$ is derived using (5) and (6), where $H_1(\beta, d_0, h, \alpha_d, \alpha_u)$ and $H_2(\beta, d_0, h, \alpha_d, \alpha_u)$ are provided in (7) and (8), respectively.

2) *Performance of UAV network:* For UAV network, the coverage probability of its typical user is

$$P_2 = P(\gamma_{uu} > \beta), \tag{22}$$

where β is SINR threshold and γ_{uu} is the SINR of the typical user in UAV network. Applying the channel model in (1), P_2 is expressed as

$$\begin{aligned}
P_2 &= P_{\text{LoS}} P\left(\frac{P_u x_0^{-\alpha_u} g_i}{I_u^c} > \beta\right) + P_{\text{NLoS}} P\left(\frac{\eta P_u x_0^{-\alpha_u} g_i}{I_u^c} > \beta\right) \\
&= P_{\text{LoS}} \exp\left(-\frac{\beta x_0^{\alpha_u} I_u^c}{P_u}\right) + (1 - P_{\text{LoS}}) \exp\left(-\frac{\beta x_0^{\alpha_u} I_u^c}{\eta P_u}\right) \\
&= P_{\text{LoS}} L_{I_u^c}\left(-\frac{\beta x_0^{\alpha_u}}{P_u}\right) + (1 - P_{\text{LoS}}) L_{I_u^c}\left(-\frac{\beta x_0^{\alpha_u}}{\eta P_u}\right),
\end{aligned} \tag{23}$$

where x_0 is the distance between the associated UAV BS and the typical user. I_u^c is the aggregated interference received by the typical user from UAVs, which is expressed as follows.

$$\begin{aligned}
I_u^c &= I_{u,\text{LoS}}^c + I_{u,\text{NLoS}}^c \\
&= \sum_{x_i \in \Phi_u \setminus \{0\}} P_{\text{LoS}} P_u x_i^{-\alpha_u} g_i + \\
&\quad \sum_{x_i \in \Phi_u \setminus \{0\}} (1 - P_{\text{LoS}}) \eta P_u x_i^{-\alpha_u} g_i.
\end{aligned} \tag{24}$$

The Laplace transform of I_u^c is

$$\begin{aligned}
L_{I_u^c}\left(\frac{\beta x_0^{\alpha_u}}{P_u}\right) &= L_{I_{u,\text{LoS}}^c}\left(\frac{\beta x_0^{\alpha_u}}{P_u}\right) L_{I_{u,\text{NLoS}}^c}\left(\frac{\beta x_0^{\alpha_u}}{P_u}\right) \\
&= E_{\Phi_u} \left[\prod_{x_i \in \Phi_u \setminus \{0\}} \frac{1}{1 + \beta x_0^{\alpha_u} P_{\text{LoS}} x_i^{-\alpha_u}} \right] \times \\
&\quad E_{\Phi_u} \left[\prod_{x_i \in \Phi_u \setminus \{0\}} \frac{1}{1 + \beta x_0^{\alpha_u} (1 - P_{\text{LoS}}) \eta x_i^{-\alpha_u}} \right].
\end{aligned} \tag{25}$$

$L_{I_{u,\text{LoS}}^c}\left(\frac{\beta x_0^{\alpha_u}}{P_u}\right)$ and $L_{I_{u,\text{NLoS}}^c}\left(\frac{\beta x_0^{\alpha_u}}{P_u}\right)$ are derived in (18) and (19), where $H_3(\beta, x_0, h, \alpha_u)$ and $H_4(\beta, x_0, h, \alpha_u)$ are provided in (20) and (21), respectively.

B. Spectrum sharing of 3D UAV network

With UAVs deployed in 3D space, height dimension needs to be considered. For the ground network, the coverage probability of typical user, denoted by P_1 , is as follows according to (12).

$$P_1 = L_{I_{gu}^c}\left(\frac{\beta d_0^{\alpha_d}}{P_d}\right) L_{I_u}\left(\frac{\beta d_0^{\alpha_d}}{P_d}\right) \exp\left(-\frac{\beta d_0^{\alpha_d} N}{P_d}\right). \tag{26}$$

$L_{I_u}\left(\frac{\beta d_0^{\alpha_d}}{P_d}\right)$ is derived in (28) and (29), where $H_5(\beta, d_0, h, \alpha_d, \alpha_u)$ and $H_6(\beta, d_0, h, \alpha_d, \alpha_u)$ are derived in (30) and (31).

For UAV network, the coverage probability of typical user is denoted by P_2 . According to (23) and (25), we have

$$\begin{aligned}
P_2 &= P_{\text{LoS}} L_{I_{u,\text{LoS}}^c}\left(\frac{\beta x_0^{\alpha_u}}{P_u}\right) L_{I_{u,\text{NLoS}}^c}\left(\frac{\beta x_0^{\alpha_u}}{P_u}\right) + \\
&\quad (1 - P_{\text{LoS}}) L_{I_{u,\text{LoS}}^c}\left(\frac{\beta x_0^{\alpha_u}}{P_u}\right) L_{I_{u,\text{NLoS}}^c}\left(\frac{\beta x_0^{\alpha_u}}{P_u}\right).
\end{aligned} \tag{27}$$

$L_{I_{u,\text{LoS}}^c}\left(\frac{\beta x_0^{\alpha_u}}{P_u}\right)$ and $L_{I_{u,\text{NLoS}}^c}\left(\frac{\beta x_0^{\alpha_u}}{P_u}\right)$ are derived in (32) and (33), where $H_7(\beta, x_0, h, \alpha_u)$ and $H_8(\beta, x_0, h, \alpha_u)$ are provided in (34) and (35), respectively.

$$\begin{aligned}
L_{I_{u,\text{LoS}}} \left(\frac{\beta d_0^{\alpha_d}}{P_d} \right) &= \exp(-\lambda_{3D_u} \int_V \left(1 - \frac{1}{1 + \frac{\beta d_0^{\alpha_d}}{P_d} P_u P_{\text{LoS}} x_i^{-\alpha_u}} \right) dx) \\
&= \exp(-2\pi \lambda_{3D_u} \int_{h_1}^{h_2} \int_0^\infty \left(1 - \frac{1}{1 + \frac{\beta d_0^{\alpha_d}}{P_d} P_u (\sqrt{r^2 + z^2})^{-\alpha_u} \frac{1}{1 + C \exp(-B(\frac{180}{\pi} \arctan(z/r) - C))}} \right) r dr dz) \quad (28) \\
&= \exp(-2\pi \lambda_{3D_u} H_5(\beta, d_0, h, \alpha_d, \alpha_u)),
\end{aligned}$$

$$\begin{aligned}
L_{I_{u,\text{NLoS}}} \left(\frac{\beta d_0^{\alpha_d}}{P_d} \right) &= \exp(-2\pi \lambda_{3D_u} \int_{h_1}^{h_2} \int_0^\infty \left(1 - \frac{1}{1 + \frac{\beta d_0^{\alpha_d}}{P_d} P_u \eta (\sqrt{r^2 + z^2})^{-\alpha_u} \left(1 - \frac{1}{1 + C \exp(-B(\frac{180}{\pi} \arctan(z/r) - C))} \right)} \right) r dr dz) \\
&= \exp(-2\pi \lambda_{3D_u} H_6(\beta, d_0, h, \alpha_d, \alpha_u)), \quad (29)
\end{aligned}$$

where

$$H_5(\beta, d_0, h, \alpha_d, \alpha_u) = \int_{h_1}^{h_2} \int_0^\infty \left(1 - \frac{1}{1 + \frac{\beta d_0^{\alpha_d}}{P_d} P_u (\sqrt{r^2 + z^2})^{-\alpha_u} \frac{1}{1 + C \exp(-B(\frac{180}{\pi} \arctan(z/r) - C))}} \right) r dr dz, \quad (30)$$

$$H_6(\beta, d_0, h, \alpha_d, \alpha_u) = \int_{h_1}^{h_2} \int_0^\infty \left(1 - \frac{1}{1 + \frac{\beta d_0^{\alpha_d}}{P_d} P_u \eta (\sqrt{r^2 + z^2})^{-\alpha_u} \left(1 - \frac{1}{1 + C \exp(-B(\frac{180}{\pi} \arctan(z/r) - C))} \right)} \right) r dr dz. \quad (31)$$

$$\begin{aligned}
L_{I_{u,\text{LoS}}}^c \left(\frac{\beta x_0^{\alpha_u}}{P_u} \right) &= \exp(-\lambda_{3D_u} \int_V \left(1 - \frac{1}{1 + \beta x_0^{\alpha_u} P_{\text{LoS}} x_i^{-\alpha_u}} \right) dx) \\
&= \exp(-\lambda_{3D_u} \int_{h_1}^{h_2} \int_0^{2\pi} \int_0^\infty \left(1 - \frac{1}{1 + \beta x_0^{\alpha_u} (\sqrt{r^2 + z^2})^{-\alpha_u} \frac{1}{1 + C \exp(-B(\frac{180}{\pi} \arctan(z/r) - C))}} \right) r dr d\phi dz) \quad (32) \\
&= \exp(-2\pi \lambda_{3D_u} H_7(\beta, x_0, h, \alpha_u)),
\end{aligned}$$

$$\begin{aligned}
L_{I_{u,\text{NLoS}}}^c \left(\frac{\beta x_0^{\alpha_u}}{P_u} \right) &= \exp(-2\pi \lambda_{3D_u} \int_{h_1}^{h_2} \int_0^\infty \left(1 - \frac{1}{1 + \beta x_0^{\alpha_u} \eta (\sqrt{r^2 + z^2})^{-\alpha_u} \left(1 - \frac{1}{1 + C \exp(-B(\frac{180}{\pi} \arctan(z/r) - C))} \right)} \right) r dr dz) \\
&= \exp(-2\pi \lambda_{3D_u} H_8(\beta, x_0, h, \alpha_u)), \quad (33)
\end{aligned}$$

where

$$H_7(\beta, x_0, h, \alpha_u) = \int_{h_1}^{h_2} \int_0^\infty \left(1 - \frac{1}{1 + \beta x_0^{\alpha_u} (\sqrt{r^2 + z^2})^{-\alpha_u} \frac{1}{1 + C \exp(-B(\frac{180}{\pi} \arctan(z/r) - C))}} \right) r dr dz, \quad (34)$$

$$H_8(\beta, x_0, h, \alpha_u) = \int_{h_1}^{h_2} \int_0^\infty \left(1 - \frac{1}{1 + \beta x_0^{\alpha_u} \eta (\sqrt{r^2 + z^2})^{-\alpha_u} \left(1 - \frac{1}{1 + C \exp(-B(\frac{180}{\pi} \arctan(z/r) - C))} \right)} \right) r dr dz. \quad (35)$$

C. Transition from 3D UAV network to 2D UAV network

In 3D UAV network, UAVs are deployed in the space with vertical range Δh . When $\Delta h \rightarrow 0$, 3D UAV network becomes 2D UAV network. In this situation, UAVs are deployed on a plane with height h_1 and area S . Supposing that the total number of UAVs is N , we have

$$L_{I_{u,\text{LoS}}}^{2D} \left(\frac{\beta x_0^{\alpha_u}}{P_u} \right) = \exp(-2\pi \frac{N}{S} f(h_1)), \quad (36)$$

and

$$L_{I_{u,\text{LoS}}}^{3D} \left(\frac{\beta x_0^{\alpha_u}}{P_u} \right) = \exp(-2\pi \frac{N}{S \cdot \Delta h} \int_{h_1}^{h_1 + \Delta h} f(z) dz). \quad (37)$$

According to L'Hôpital's rule, we have

$$\begin{aligned}
L_{I_{u,\text{LoS}}}^{3D} \left(\frac{\beta x_0^{\alpha_u}}{P_u} \right) &\stackrel{\Delta h \rightarrow 0}{=} \exp(-2\pi \frac{N}{S \cdot \Delta h} \int_{h_1}^{h_1 + \Delta h} f(z) dz) \\
&\stackrel{\Delta h \rightarrow 0}{=} \exp(-2\pi \frac{N}{S} f(h_1)) \\
&\stackrel{\Delta h \rightarrow 0}{=} L_{I_{u,\text{LoS}}}^{2D} \left(\frac{\beta x_0^{\alpha_u}}{P_u} \right). \quad (38)
\end{aligned}$$

According to (38), when $\Delta h \rightarrow 0$, the coverage probabilities with 3D UAV deployment tend to the results with 2D UAV deployment.

IV. SPECTRUM SHARING WITH DIRECTIONAL TRANSMISSION

In this section, directional transmission is considered to improve the performance of spectrum sharing. Antenna gain is provided in (3).

1) *Spectrum sharing of 2D UAV network*: When UAV adopts directional transmission, I_{gu}^c is (10) and P_1 is (12). Then I_u is derived as follows.

$$\begin{aligned} I_u &= I_{u,\text{LoS}} + I_{u,\text{NLoS}} \\ &= \sum_{x_i \in \Phi_u} P_{\text{LoS}} P_u x_i^{-\alpha_d} g_i G(\varphi_i) + \\ &\quad \sum_{x_i \in \Phi_u} (1 - P_{\text{LoS}}) \eta P_u x_i^{-\alpha_d} g_i G(\varphi_i). \end{aligned} \quad (39)$$

Then $L_{I_{u,\text{LoS}}}\left(\frac{\beta d_0^{\alpha_d}}{P_d}\right)$ and $L_{I_{u,\text{NLoS}}}\left(\frac{\beta d_0^{\alpha_d}}{P_d}\right)$ are modified as follows.

$$\begin{aligned} L_{I_{u,\text{LoS}}}\left(\frac{\beta d_0^{\alpha_d}}{P_d}\right) &= E_{I_{u,\text{LoS}}}\left[\exp\left(\frac{\beta d_0^{\alpha_d}}{P_d} I_{u,\text{LoS}}\right)\right] \\ &= E_{\Phi_u}\left[\prod_{x_i \in \Phi_u \setminus \{0\}} \frac{1}{1 + \frac{\beta d_0^{\alpha_d}}{P_d} P_u P_{\text{LoS}} x_i^{-\alpha_u} G(\varphi_i)}\right]. \quad (40) \\ L_{I_{u,\text{NLoS}}}\left(\frac{\beta d_0^{\alpha_d}}{P_d}\right) &= E_{\Phi_u}\left[\prod_{x_i \in \Phi_u \setminus \{0\}} \frac{1}{1 + \frac{\beta d_0^{\alpha_d}}{P_d} P_u (1 - P_{\text{LoS}}) \eta x_i^{-\alpha_u} G(\varphi_i)}\right]. \quad (41) \end{aligned}$$

$L_{I_{u,\text{LoS}}}\left(\frac{\beta d_0^{\alpha_d}}{P_d}\right)$ and $L_{I_{u,\text{NLoS}}}\left(\frac{\beta d_0^{\alpha_d}}{P_d}\right)$ can be derived using the probability generation function in (44) and (45), where $H_9(\beta, d_0, h, \alpha_u)$ and $H_{10}(\beta, d_0, h, \alpha_u)$ are provided in (46) and (47), respectively.

For UAV network user, we have

$$\begin{aligned} I_u^c &= I_{u,\text{LoS}}^c + I_{u,\text{NLoS}}^c \\ &= \sum_{x_i \in \Phi_u \setminus \{0\}} P_{\text{LoS}} P_u x_i^{-\alpha_d} g_i G(\phi_i) + \\ &\quad \sum_{x_i \in \Phi_u \setminus \{0\}} (1 - P_{\text{LoS}}) \eta P_u x_i^{-\alpha_d} g_i G(\phi_i), \end{aligned} \quad (42)$$

$$\begin{aligned} L_{I_u^c}\left(\frac{\beta x_0^{\alpha_u}}{P_u G(\phi_0)}\right) &= L_{I_{u,\text{LoS}}^c}\left(\frac{\beta x_0^{\alpha_u}}{P_u G(\phi_0)}\right) L_{I_{u,\text{NLoS}}^c}\left(\frac{\beta x_0^{\alpha_u}}{P_u G(\phi_0)}\right) \\ &= E_{\Phi_u}\left[\prod_{x_i \in \Phi_u \setminus \{0\}} \frac{1}{1 + \beta x_0^{\alpha_u} P_{\text{LoS}} x_i^{-\alpha_u} \frac{G(\phi_i)}{G(\phi_0)}}\right] \times \\ & E_{\Phi_u}\left[\prod_{x_i \in \Phi_u \setminus \{0\}} \frac{1}{1 + \beta x_0^{\alpha_u} (1 - P_{\text{LoS}}) \eta x_i^{-\alpha_u} \frac{G(\phi_i)}{G(\phi_0)}}\right]. \end{aligned} \quad (43)$$

$L_{I_{u,\text{LoS}}^c}\left(\frac{\beta x_0^{\alpha_u}}{P_u G(\phi_0)}\right)$ and $L_{I_{u,\text{NLoS}}^c}\left(\frac{\beta x_0^{\alpha_u}}{P_u G(\phi_0)}\right)$ can be derived using the probability generation function in (48) and (49), where

TABLE II
SIMULATION PARAMETERS

Parameter	Value
P_u	5 W
P_d	0.1 W
α_u	3
α_d	4
B and C	0.136 and 11.95
β	0.1
η	0.001
λ_u	10^{-4} per square meter
λ_d	10^{-3} per square meter
d_0	10 m
N	10^{-9} W

$H_{11}(\beta, x_0, h, \alpha_u)$ and $H_{12}(\beta, x_0, h, \alpha_u)$ are provided in (50) and (51), respectively.

2) *Spectrum sharing of 3D UAV network*: For ground network user, $L_{I_{u,\text{LoS}}}\left(\frac{\beta d_0^{\alpha_d}}{P_d}\right)$ and $L_{I_{u,\text{NLoS}}}\left(\frac{\beta d_0^{\alpha_d}}{P_d}\right)$ can be obtained using the probability generation function in (52) and (53), where $H_{13}(\beta, d_0, h, \alpha_u)$ and $H_{14}(\beta, d_0, h, \alpha_u)$ are provided in (54) and (55), respectively.

For UAV network user, $L_{I_{u,\text{LoS}}^c}\left(\frac{\beta x_0^{\alpha_u}}{P_u G(\phi_0)}\right)$ and $L_{I_{u,\text{NLoS}}^c}\left(\frac{\beta x_0^{\alpha_u}}{P_u G(\phi_0)}\right)$ can be derived using the probability generation function in (56) and (57), where $H_{15}(\beta, x_0, h, \alpha_u)$ and $H_{16}(\beta, x_0, h, \alpha_u)$ are derived in (58) and (59).

V. SIMULATION RESULTS AND ANALYSIS

In this section, the simulation results regarding the performance of UAV network and ground network with spectrum sharing are provided. The main parameters for simulation are summarized in Table II.

A. The performance of ground network user

1) *Omnidirectional A2A transmission*: P_1 is illustrated in Fig. 4 and Fig. 5. The Monte Carlo results, each of which runs 10^6 times simulations, are provided. The solid lines denoting the theoretical results fit well with the points denoting the Monte Carlo results. In Fig. 4, P_1 is a unimodal function of h . When h is smaller than a threshold, the increase of h will result in the increase of the probability of LoS transmission, which will decrease P_1 . However, when h is larger than a threshold, the increase of h will enlarge the distance between UAVs and the typical user of ground network, which will increase P_1 . In Fig. 4, with the increase of λ_u , the interference from UAVs to the typical user of ground network increases. As a result, the coverage probability of ground network user decreases in this situation.

Fig. 5 illustrates P_1 versus h_1 with 3D UAV deployment. P_1 is also a unimodal function of h . On the other hand, P_1 is a decreasing function of Δh .

2) *Directional A2A transmission*: P_1 versus height with 2D and 3D UAV deployment is illustrated in Fig. 6 and Fig. 7. Comparing Fig. 6 and Fig. 7 with Fig. 4 and Fig. 5, respectively, we discover that P_1 with directional transmission is

$$\begin{aligned}
L_{I_{u,\text{LoS}}}(\frac{\beta d_0^{\alpha_d}}{P_d}) &= \exp(-\lambda_2 D_u \int_V (1 - \frac{1}{1 + \frac{\beta d_0^{\alpha_d}}{P_d} P_u P_{\text{LoS}} x_i^{-\alpha_u} G(\varphi_i)}) dx) \\
&= \exp(-2\pi \lambda_2 D_u \int_0^\infty (1 - \frac{1}{1 + \frac{\beta d_0^{\alpha_d}}{P_d} P_u (\sqrt{r^2 + h^2})^{-\alpha_u} G(\arctan(r/h)) \frac{1}{1+C \exp(-B(\frac{180}{\pi} \arctan(h/r)-C))}}) r dr) \\
&= \exp(-2\pi \lambda_2 D_u H_9(\beta, d_0, h, \alpha_d, \alpha_u)),
\end{aligned} \tag{44}$$

$$L_{I_{u,\text{NLoS}}}(\frac{\beta d_0^{\alpha_d}}{P_d}) = \exp(-2\pi \lambda_2 D_u H_{10}(\beta, d_0, h, \alpha_d, \alpha_u)), \tag{45}$$

where

$$H_9(\beta, d_0, h, \alpha_d, \alpha_u) = \int_0^\infty (1 - \frac{1}{1 + \frac{\beta d_0^{\alpha_d}}{P_d} P_u (\sqrt{r^2 + h^2})^{-\alpha_u} G(\arctan(r/h)) \frac{1}{1+C \exp(-B(\frac{180}{\pi} \arctan(h/r)-C))}}) r dr, \tag{46}$$

$$H_{10}(\beta, d_0, h, \alpha_d, \alpha_u) = \int_0^\infty (1 - \frac{1}{1 + \frac{\beta d_0^{\alpha_d}}{P_d} P_u (\sqrt{r^2 + h^2})^{-\alpha_u} \eta G(\arctan(r/h)) (1 - \frac{1}{1+C \exp(-B(\frac{180}{\pi} \arctan(h/r)-C))})}) r dr. \tag{47}$$

$$\begin{aligned}
L_{I_{u,\text{LoS}}^c}(\frac{\beta x_0^{\alpha_u}}{P_u G(\phi_0)}) &= \exp(-\lambda_2 D_u \int_V (1 - \frac{1}{1 + \beta x_0^{\alpha_u} P_{\text{LoS}} x_i^{-\alpha_u} \frac{G(\phi_i)}{G(\phi_0)}}) dx) \\
&= \exp(-2\pi \lambda_2 D_u \int_0^\infty (1 - \frac{1}{1 + \beta x_0^{\alpha_u} (\sqrt{r^2 + h^2})^{-\alpha_u} \frac{G(\arctan(r/h))}{G(\phi_0)} \frac{1}{1+C \exp(-B(\frac{180}{\pi} \arctan(h/r)-C))}}) r dr) \\
&= \exp(-2\pi \lambda_2 D_u H_{11}(\beta, x_0, h, \alpha_u)),
\end{aligned} \tag{48}$$

$$L_{I_{u,\text{NLoS}}^c}(\frac{\beta x_0^{\alpha_u}}{P_u G(\phi_0)}) = \exp(-2\pi \lambda_2 D_u H_{12}(\beta, x_0, h, \alpha_u)), \tag{49}$$

where

$$H_{11}(\beta, x_0, h, \alpha_u) = \int_0^\infty (1 - \frac{1}{1 + \beta x_0^{\alpha_u} (\sqrt{r^2 + h^2})^{-\alpha_u} \frac{G(\arctan(r/h))}{G(\phi_0)} \frac{1}{1+C \exp(-B(\frac{180}{\pi} \arctan(h/r)-C))}}) r dr, \tag{50}$$

$$H_{12}(\beta, x_0, h, \alpha_u) = \int_0^\infty (1 - \frac{1}{1 + \beta x_0^{\alpha_u} (\sqrt{r^2 + h^2})^{-\alpha_u} \eta \frac{G(\arctan(r/h))}{G(\phi_0)} (1 - \frac{1}{1+C \exp(-B(\frac{180}{\pi} \arctan(h/r)-C))})}) r dr. \tag{51}$$

larger than that with omnidirectional transmission. According to Fig. 4 and Fig. 5, the coverage probability of the typical user in ground network with directional transmission is larger than that with omnidirectional transmission.

B. The performance of UAV network user

1) *Omnidirectional A2G transmission:* P_2 is illustrated in Fig. 8 and Fig. 9. The Monte Carlo results, each of which runs 10^6 times simulations, are provided. The lines denoting the theoretical results fit well with the dots denoting Monte Carlo results. For 2D and 3D UAV networks, there exists optimal height to maximize P_2 . When UAVs are 2D deployed, P_2 is inversely proportional to the increase of UAVs' density because users of typical UAV network receive increasing interference. When UAVs are 3D deployed, P_2 is proportional to the increase of Δh because the interference received by

the typical UAV network user from interfering UAVs will decrease.

2) *Directional A2G transmission:* With directional A2G communication, P_2 can be improved. Comparing Fig. 8 with Fig. 10, it can be found that for 2D UAV deployment, P_2 with directional A2G transmission is larger than that with omnidirectional A2G transmission, especially in the situation with large heights. The essential reason is that when a UAV is high above ground and adopts omnidirectional A2G transmission, UAV can generate interference to a large number of UAV network users. However, with directional A2G transmission, UAV will generate interference to a relatively limited number of UAV network users. Similarly, comparing Fig. 9 with Fig. 11, it can be discovered that for 3D UAV network, P_2 with directional A2G transmission is still larger than that with omnidirectional A2G transmission especially when h_1 is large.

$$L_{I_{u,\text{LoS}}}\left(\frac{\beta d_0^{\alpha_d}}{P_d}\right) = \exp(-\lambda_{3Du} \int_V \left(1 - \frac{1}{1 + \frac{\beta d_0^{\alpha_d}}{P_d} P_u P_{\text{LoS}} x_i^{-\alpha_u} G(\varphi_i)}\right) dx) = \exp(-2\pi\lambda_{3Du} H_{13}(\beta, d_0, h, \alpha_d, \alpha_u)), \quad (52)$$

$$L_{I_{u,\text{NLoS}}}\left(\frac{\beta d_0^{\alpha_d}}{P_d}\right) = \exp(-2\pi\lambda_{3Du} H_{14}(\beta, d_0, h, \alpha_d, \alpha_u)), \quad (53)$$

where

$$H_{13}(\beta, d_0, h, \alpha_d, \alpha_u) = \int_{h_1}^{h_2} \int_0^\infty \left(1 - \frac{1}{1 + \frac{\beta d_0^{\alpha_d}}{P_d} P_u (\sqrt{r^2 + z^2})^{-\alpha_u} G(\arctan(r/z)) \frac{1}{1+C \exp(-B(\frac{180}{\pi} \arctan(z/r)-C))}}\right) r dr dz, \quad (54)$$

$$H_{14}(\beta, d_0, h, \alpha_d, \alpha_u) = \int_{h_1}^{h_2} \int_0^\infty \left(1 - \frac{1}{1 + \frac{\beta d_0^{\alpha_d}}{P_d} P_u \eta (\sqrt{r^2 + z^2})^{-\alpha_u} G(\arctan(r/z)) \left(1 - \frac{1}{1+C \exp(-B(\frac{180}{\pi} \arctan(z/r)-C))}\right)}\right) r dr dz. \quad (55)$$

$$L_{I_{u,\text{LoS}}^c}\left(\frac{\beta x_0^{\alpha_u}}{P_u G(\phi_0)}\right) = \exp(-\lambda_{3Du} \int_V \left(1 - \frac{1}{1 + \beta x_0^{\alpha_u} P_{\text{LoS}} x_i^{-\alpha_u} \frac{G(\phi_i)}{G(\phi_0)}}\right) dx) = \exp(-2\pi\lambda_{3Du} H_{15}(\beta, x_0, h, \alpha_u)), \quad (56)$$

$$L_{I_{u,\text{NLoS}}^c}\left(\frac{\beta x_0^{\alpha_u}}{P_u}\right) = \exp(-2\pi\lambda_{3Du} H_{16}(\beta, x_0, h, \alpha_u)), \quad (57)$$

where

$$H_{15}(\beta, x_0, h, \alpha_u) = \int_{h_1}^{h_2} \int_0^\infty \left(1 - \frac{1}{1 + \beta x_0^{\alpha_u} (\sqrt{r^2 + z^2})^{-\alpha_u} \frac{G(\arctan(r/z))}{G(\phi_0)} \frac{1}{1+C \exp(-B(\frac{180}{\pi} \arctan(z/r)-C))}}\right) r dr dz, \quad (58)$$

$$H_{16}(\beta, x_0, h, \alpha_u) = \int_{h_1}^{h_2} \int_0^\infty \left(1 - \frac{1}{1 + \beta x_0^{\alpha_u} \eta (\sqrt{r^2 + z^2})^{-\alpha_u} \frac{G(\arctan(r/z))}{G(\phi_0)} \left(1 - \frac{1}{1+C \exp(-B(\frac{180}{\pi} \arctan(z/r)-C))}\right)}\right) r dr dz. \quad (59)$$

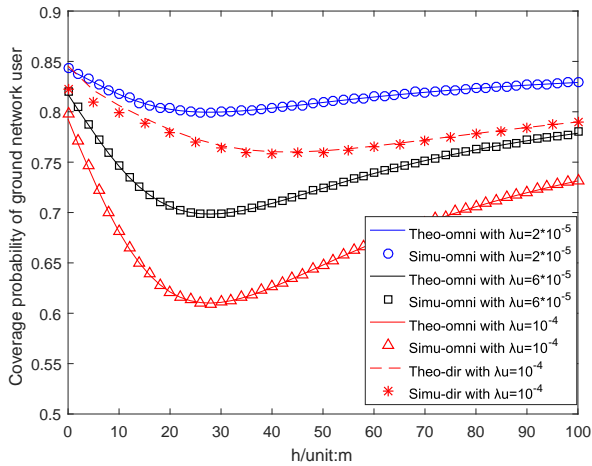


Fig. 4. The coverage probability of ground network user versus h for 2D UAV deployment and omnidirectional A2A transmission, where “theo/simu-omni/dir” refers to theoretical/simulation results of omni/directional A2A transmission.

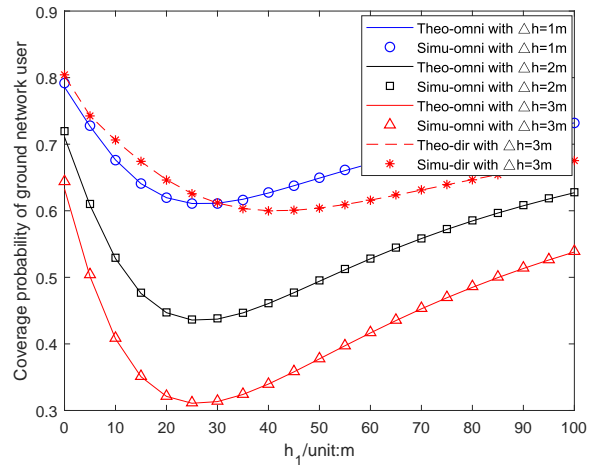


Fig. 5. The coverage probability of ground network user versus h_1 for 3D UAV deployment and omnidirectional A2A transmission, where “theo/simu-omni/dir” refers to theoretical/simulation results of omni/directional A2A transmission.

C. Optimal height of UAVs

The concept of transmission capacity (TC) is adopted as the performance metric of UAV network, which is as follows [14].

$$T_u = \lambda_u P(\gamma_{uu} > \beta) \log(1 + \beta), \quad (60)$$

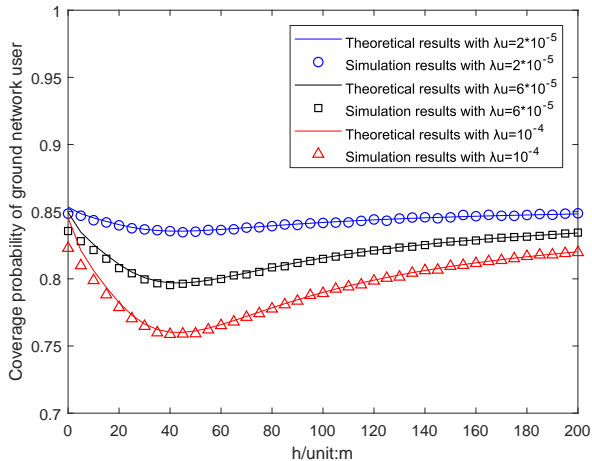


Fig. 6. The coverage probability of ground network user versus h for 2D UAV deployment and directional A2A transmission.

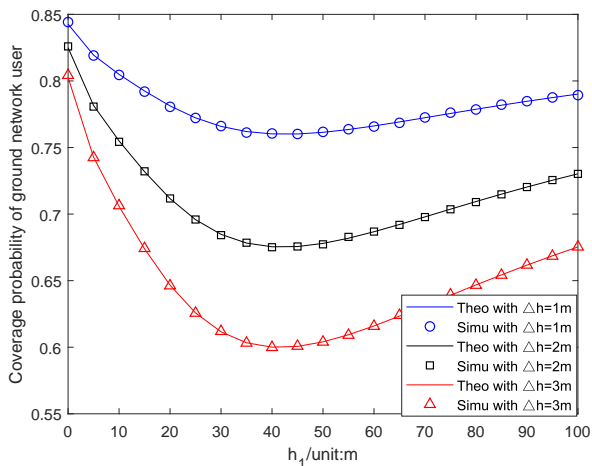


Fig. 7. The coverage probability of ground network user versus h_1 for 3D UAV deployment and directional A2A transmission, where “theo/simu” refers to theoretical/simulation results.

where γ_{uu} denotes SINR. In this paper, transmission capacity T_u refers to the sum capacity of UAV network users per unit area which can successful communication. Solving the optimization model as follows, the optimal altitude of UAVs could be obtained.

$$\begin{aligned} \max_h T_u \\ \text{s.t. } P_1 \geq \alpha. \end{aligned} \quad (61)$$

Since the inequalities in (61) is complex, the closed-form solution is hard to be obtained. The optimal solution can be searched numerically.

TC of 2D UAV network is illustrated in Fig. 12. TC of UAV network is an increasing function of the density of UAVs. Besides, the directional transmission can improve TC of UAV network. Considering TC of UAV network changing with h , there exists an optimal h to maximize the TC of UAV network. However, when λ_u is highest in simulation, for example, $\lambda_u = 10^{-4}$ and omnidirectional transmission is adopted, there is a vacant interval of h , where the interference received by the

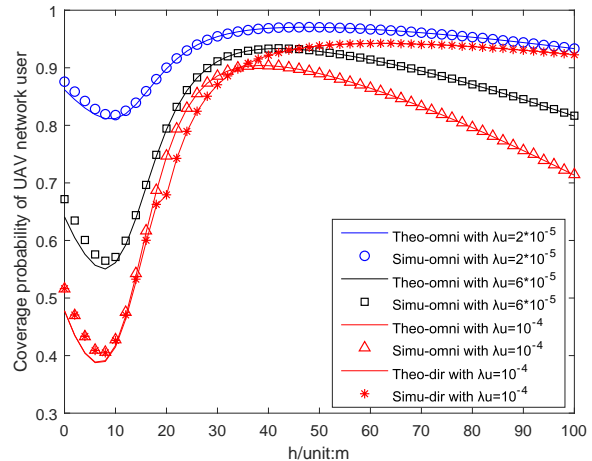


Fig. 8. The coverage probability of UAV network user versus h for 2D UAV deployment and omnidirectional A2A transmission, where “theo/simu-omni/dir” refers to theoretical/simulation results of omni/directional A2A transmission.

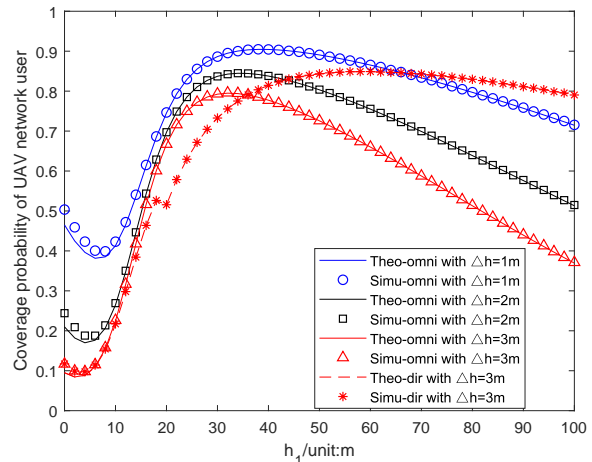


Fig. 9. The coverage probability of UAV network user versus h_1 for 3D UAV deployment and omnidirectional A2A transmission, where “theo/simu-omni/dir” refers to theoretical/simulation results of omni/directional A2A transmission.

ground network user from UAVs is large and the constraint in (61) is not satisfied. Hence, there exists a vacant interval in the curve, which is denoted by a circle in Fig. 12.

In Fig. 13, TC of 3D UAV network is decreasing with the increase of Δh . Meanwhile, the directional transmission improves TC of UAV network. Similar to 2D UAV network, there exist vacant intervals for the curves of TC of 3D UAV network, where the interference received by ground network user from UAVs is small and the constraint of (61) is not satisfied.

VI. CONCLUSION

In this paper, the spectrum sharing between UAV enabled wireless mesh networks and ground networks is analyzed using stochastic geometry. The correctness of theoretical derivation is verified by simulation results. When $\Delta h \rightarrow 0$,

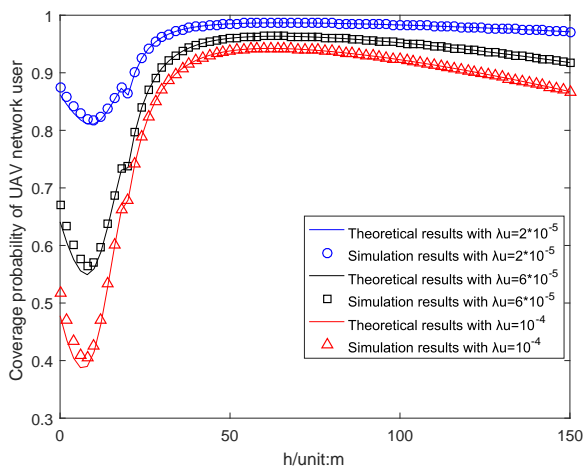


Fig. 10. The coverage probability of UAV network user versus h for 2D UAV network and directional transmission.

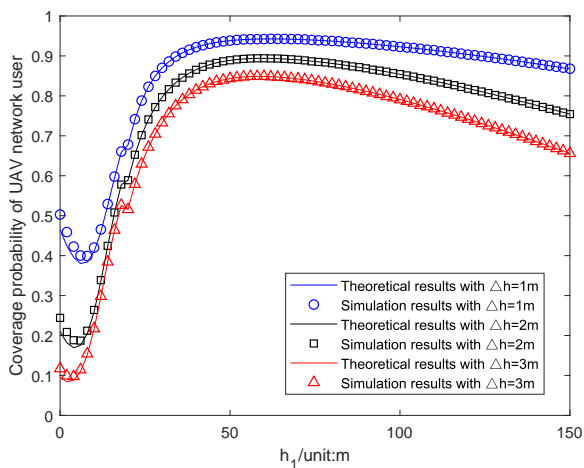


Fig. 11. The coverage probability of UAV network user versus h_1 for 3D UAV network and directional transmission.

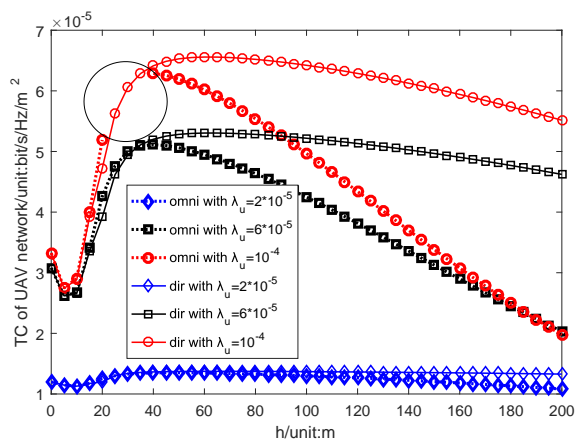


Fig. 12. The transmission capacity of UAV network user versus h for 2D UAV network, where “omni/dir” refers to omnidirectional/directional A2A transmission.

the derived results of 3D UAV network reduce to that of

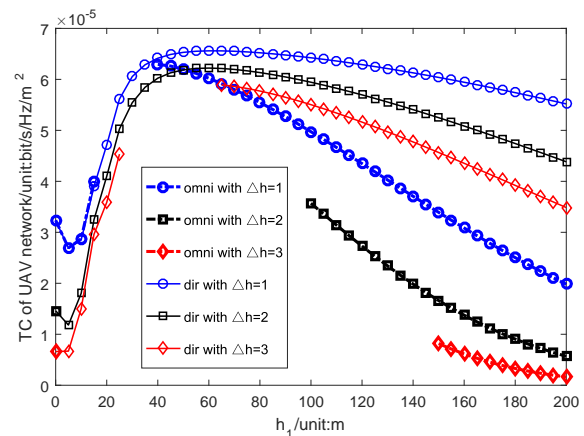


Fig. 13. The transmission capacity of UAV network user versus Δh for 3D UAV network, where “omni/dir” refers to omnidirectional/directional A2A transmission.

2D UAV network. This is also verified in simulation results. Compared with omnidirectional transmission, the performance of spectrum sharing with directional transmission is better. We can find the optimal height of UAVs achieved to maximize the transmission capacity within the constraint of the coverage probability of ground network user. This paper provides performance analysis of UAV network, which may motivate the study of architecture, protocol and resource allocation for aerial wireless mesh networks with spectrum sharing.

REFERENCES

- [1] B. Li, Z. Fei, and Y. Zhang, “UAV Communications for 5G and Beyond: Recent Advances and Future Trends,” *IEEE Internet of Things Journal*, vol. 6, no. 2, pp. 2241–2263, Apr. 2019.
- [2] M. Erdelj, E. Natalizio, K. R. Chowdhury, and I. F. Akyildiz, “Help from the Sky: Leveraging UAVs for Disaster Management,” *IEEE Pervasive Computing*, vol. 16, no. 1, pp. 24–32, Jan.-Mar. 2017.
- [3] H. Wu, X. Tao, N. Zhang, and X. Shen, “Cooperative UAV Cluster-Assisted Terrestrial Cellular Networks for Ubiquitous Coverage,” *IEEE Journal on Selected Areas in Communications*, vol. 36, no. 9, pp. 2045–2058, Sept. 2018.
- [4] P. Zhou, X. Fang, Y. Fang, R. He, Y. Long, and G. Huang, “Beam Management and Self-Healing for mmWave UAV Mesh Networks,” *IEEE Transactions on Vehicular Technology*, vol. 68, no. 2, pp. 1718–1732, Feb. 2019.
- [5] M. Sbeiti, N. Goddemeier, D. Behnke, and C. Wietfeld, “PASER: Secure and Efficient Routing Approach for Airborne Mesh Networks,” *IEEE Transactions on Wireless Communications*, vol. 15, no. 3, pp. 1950–1964, Mar. 2016.
- [6] J. Lyu, Y. Zeng, R. Zhang, and T. J. Lim, “Placement Optimization of UAV-Mounted Mobile Base Stations,” *IEEE Communications Letters*, vol. 21, no. 3, pp. 604–607, Mar. 2017.
- [7] I. Bor-Yaliniz, S. S. Szyszkowicz, and H. Yanikomeroglu, “Environment-Aware Drone-Base-Station Placements in Modern Metropolitan,” *IEEE Wireless Communications Letters*, vol. 7, no. 3, pp. 372–375, Jun. 2018.
- [8] J. Plachy, Z. Becvar, P. Mach, R. Marik, and M. Vondra, “Joint Positioning of Flying Base Stations and Association of Users: Evolutionary-Based Approach,” *IEEE Access*, vol. 7, pp. 11454–11463, Jan. 2019.
- [9] N. Lu, Y. Zhou, C. Shi, N. Cheng, L. Cai, and B. Li, “Planning While Flying: A Measurement-Aided Dynamic Planning of Drone Small Cells,” *IEEE Internet of Things Journal*, vol. 6, no. 2, pp. 2693–2705, Apr. 2019.
- [10] Y. Wang, Z. Wei, X. Chen, H. Wu, Z. Feng, “Demo: UAV Assisted Adaptive Aerial Internet,” In *Proceedings of IEEE/CIC International Conference on Communications in China (ICCC)*, pp. 1–2, Beijing, China, Aug. 2018.
- [11] P. Gupta and P. R. Kumar, “The capacity of wireless networks,” *IEEE Transactions on Information Theory*, vol. 46, no. 2, pp. 388–404, Mar. 2000.

- [12] Z. Wei, H. Wu, Z. Feng, and S. Chang, "Capacity of UAV Relaying Networks," *IEEE Access*, vol. 7, pp. 27207–27216, Jan. 2019.
- [13] P. Jacob, R. P. Sirigina, A. S. Madhukumar, and V. A. Prasad, "Cognitive Radio for Aeronautical Communications: A Survey," *IEEE Access*, vol. 4, pp. 3417–3443, May 2016.
- [14] C. Zhang and W. Zhang, "Spectrum Sharing for Drone Networks," *IEEE Journal on Selected Areas in Communications*, vol. 35, no. 1, pp. 136–144, Jan. 2017.
- [15] C. Zhang, Z. Wei, Z. Feng, W. Zhang, "Spectrum Sharing of Drone Networks," *Handbook of Cognitive Radio*, Springer, 2019.
- [16] J. Lyu, Y. Zeng, and R. Zhang, "Spectrum Sharing and Cyclical Multiple Access in UAV-Aided Cellular Offloading," In *Proceedings of IEEE Global Communications Conference (GLOBECOM)*, pp. 1–6, Singapore, Dec. 2017.
- [17] K. Yoshikawa, S. Yamashita, K. Yamamoto, T. Nishio, M. Morikura, "Resource Allocation for 3D Drone Networks Sharing Spectrum Bands," In *Proceedings of IEEE Vehicular Technology Conference (VTC-Fall)*, Toronto, ON, Canada, pp. 1–5, Toronto, Sept. 2017.
- [18] L. Sboui, H. Ghazzai, Z. Rezeki, M.-S. Alouini, "Energy-Efficient Power Allocation for UAV Cognitive Radio Systems," In *Proceedings of IEEE Vehicular Technology Conference (VTC-Fall)*, pp. 1–5, Toronto, ON, Canada, Sept. 2017.
- [19] X. Huang, G. Wang, F. Hu, and S. Kumar, "Stability-Capacity-Adaptive Routing for High-Mobility Multihop Cognitive Radio Networks," *IEEE Transactions on Vehicular Technology*, vol. 60, no. 6, pp. 2714–2729, Jul. 2011.
- [20] H. Wang, J. Wang, G. Ding, J. Chen, Y. Li, and Z. Han, "Spectrum Sharing Planning for Full-Duplex UAV Relaying Systems With Underlaid D2D Communications," *IEEE Journal on Selected Areas in Communications*, vol. 36, no. 9, pp. 1986–1999, Sept. 2018.
- [21] A. Hourani, K. Sithamparanathan, and S. Lardner, "Optimal LAP altitude for maximum coverage," *IEEE Wireless Communications Letters*, vol. 3, no. 6, pp. 569–572, Dec. 2014.
- [22] T. S. I. Toyoda and K. Iiguse, "Reference antenna model with side lobe for tg3c evaluation," IEEE document, 2006.
- [23] Y. Liu, Z. Feng, Z. Wei, Z. Feng, "SINR-based scheduling in multi-path multi-hop multi-radio multi-channel mmWave WPANs," *EURASIP Journal on Wireless Communications and Networking*, vol. 66, Mar. 2018.
- [24] M. Mozaffari, W. Saad, M. Bennis, and M. Debbah, "Unmanned Aerial Vehicle with Underlaid Device-to-Device Communications: Performance and Tradeoffs," *IEEE Transactions on Wireless Communications*, vol. 15, no. 6, pp. 3949–3963, Jun. 2016.
- [25] M. Haenggi and R. K. Ganti, "Interference in Large Wireless Networks," *Now Publishers Inc.*, pp. 127–248, 2009.
- [26] Z. Wei, Z. Guo, Z. Feng, J. Zhu, C. Zhong, Q. Wu, H. Wu, "Spectrum Sharing between UAV-based Wireless Mesh Networks and Ground Networks," In *Proceedings of 10th International Conference on Wireless Communications and Signal Processing (WCSP)*, Hangzhou, China, pp. 1–6, Oct. 2018.